JACS
JOURNAL OF THE AMERICAN CHEMICAL SOCIETY

Article

pubs.acs.org/JACS

Facile Separation of Regioisomeric Compounds by a Heteronuclear Organometallic Capsule

Wen-Ying Zhang, Yue-Jian Lin, Ying-Feng Han,* and Guo-Xin Jin*

Department of Chemistry, Fudan University, 220 Handan Road, 200433 Shanghai, China

Supporting Information

ABSTRACT: Owing to the often-similar physical and chemical properties of structural isomers of organic molecules, large efforts have been made to develop efficient strategies to isolate specific isomers. However, facile separation of regioisomeric compounds remains difficult. Here we demonstrate a universal organometallic capsule in which two silver centers are rigidly separated from each other by two tetranuclear [Rh_4] pyramidal frustums, which selectively encapsulate a specific isomer from mixtures. Not only is the present heterometallic capsule suitable as a host for the encapsulation of a series of aromatic compounds, but also the receptor shows widely differing specificity for the various isomers. Direct experimental evidence is provided for the selective encapsulation of a series of *para* (*p*)-disubstituted benzene derivatives, such as *p*-xylene, *p*-dichlorobenzene, *p*-dibromobenzene, and *p*-diiodobenzene. The size and shape matching, as well as the Ag−π interactions, are the main forces governing the extent of molecular recognition. The encapsulated guest *p*-xylene can be released by using the solid−liquid solvent washing strategy, and the other guest molecules are easily liberated by using light stimulus.

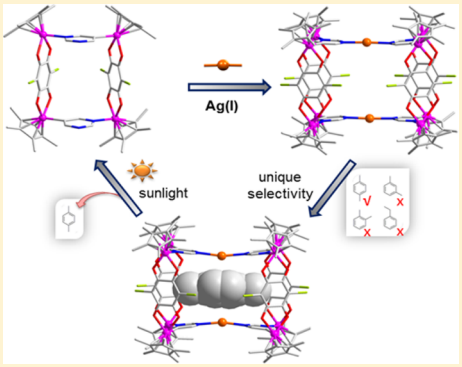

INTRODUCTION

Separation of constitutional isomers—molecules that differ in the spatial arrangement of their atoms with the same chemical formula—is an active area of research, as often each isomer can be subsequently applied to different industrial applications. However, the separation of isomeric compounds remains difficult due to their (usually) extremely similar chemical and physical properties.[1] One promising way to separate such mixtures is by using porous materials with different pore sizes and shapes. Recently, porous coordination polymers and metal−organic frameworks have been explored to separate isomeric mixtures.[2−12] In this context, approaches to the separation of C_8-alkylaromatic compounds, which exist as four possible isomeric forms (*ortho*-xylene (*o*X), *meta*-xylene (*m*X), *para*-xylene (*p*X), and ethylbenzene), have been investigated extensively.[13−27] Even now, high selectivity is usually difficult to achieve because the dimension modulation and binding site functionalization of the container used for selective accommodation of different isomers is challenging due to the limitations of controllable synthesis.

A range of discrete supramolecular capsules possessing nanospace have been designed and constructed, with an emphasis on their abilities to encapsulate guest molecules and to serve as molecular containers for chemical reactions.[28−35] The shape and size of such architectures can be precisely controlled by judicious selection of organic ligands and geometrically prefixed metal ions.[36−40] In particular, assemblies containing coordinatively labile sites at the metal center(s) have great potential for metal-mediated multipoint recognition and selective binding of target substrates.[40−48] Based on the success of many supramolecular cages and capsules and their applications in host−guest chemistry, we wished to design a single molecular capsule that not only can serve as a host for guest encapsulation but also can be used as a platform for the separation of isomeric compounds. The Ag−π interaction is a typical example of binding between a metal and an aromatic system, and has been utilized to facilitate the formation of metal ion−aromatic complexes.[49,50] The formation of xylene−silver complexes through the π-interaction of aromatic rings with silver(I) has also been reported.[51] Recently, a dinuclear macrocycle possessing a nanocavity with two coordinatively labile silver(I) centers was used for guest encapsulation, taking advantage of Ag−π interactions.[50] Therefore, we envisioned that a molecular capsule possessing a nanocavity with two silver(I) centers could be used as a new class of molecular receptor whereby the isomeric compounds can be separated through multipoint recognition of the selected guest molecules. Hence, silver ions were selected as the metal "hinges" to connect our two tetranuclear [Rh_4] pyramidal frustums. We report herein an organometallic capsule with a high inclusive selectivity for the encapsulation of *para*-disubstituted (dialkyl or dihalo) benzene derivatives and their separation from the corresponding regioisomeric mixtures. The assembly's facile ability to release the molecules using a solid−liquid solvent

Received: June 27, 2016
Published: July 27, 2016

DOI: 10.1021/jacs.6b06622
J. Am. Chem. Soc. 2016, 138, 10700−10707

washing strategy or efficient external stimulus—light has also been observed.

RESULTS AND DISCUSSION

Synthesis and Characterization of a Stable Heteroarylrhodium(III) Metallacycle by Transmetalation. A solution of dirhodium dication **2** (Figure S1 in the Supporting Information), generated in situ by chloride abstraction of $[Cp^*_2Rh_2(\mu\text{-CA})]Cl_2$ (**1**, H_2CA = chloranilic acid) with AgOTf in methanol/H_2O (10/1),[52] reacts with excess 4-pyridinylboronic acid, leading to exclusive formation of the tetranuclear metallacycle **3** (Scheme 1), formulated as

Scheme 1. Synthesis of Heteroarylrhodium Metallarectangles 3

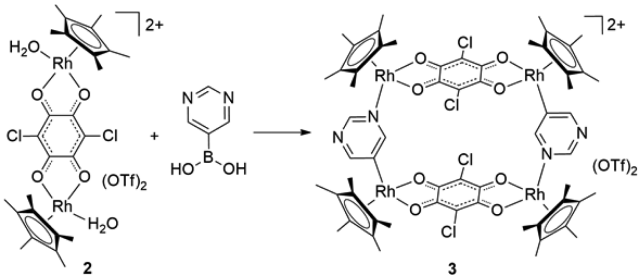

$[Cp^*_4Rh_4(\mu\text{-CA})_2(\mu\text{-C,N-pyrimidine})_2](OTf)_2$, as confirmed by NMR, elemental analysis, MALDI-TOF mass spectrometry, and single-crystal X-ray crystallography (vide infra). The selective transmetalation from boron to rhodium and coordination-driven self-assembly occurred simultaneously.[53] Dark-red crystals of complex **3** were isolated in 82% yield upon recrystallization by diffusion of diethyl ether into the red filtrate containing the complex. Multiple ^{1}H NMR resonances of the Cp* rings suggested chemically inequivalent Cp*Rh(III) centers (see below, Figure 2a). A MALDI-TOF mass spectrum with a signal at m/z = 1673, corresponding to $[\mathbf{3} - \text{OTf}]^+$, confirmed the discrete assembly of complexes **3** (Figure S2).

The single-crystal X-ray crystallographic analysis unambiguously established the structure of **3** to be a discrete metallarectangle, constructed via the formation of Rh−C bonds, indicating that the reaction involved transmetalation of the pyrimidinyl group from boron to rhodium. As shown in Figure 1, the X-ray structure revealed that two pyrimidine units are connected to metal centers with a *meta*-C,N bridging coordination mode, with one "naked" nitrogen atom remaining in each pyrimidine unit. It is noteworthy that the carbon and nitrogen atoms which coordinate to the metal centers are strongly disordered. While the two opposing pyrimidine rings are nearly face-to-face and parallel, the two bridging 2,5-dichloro-3,6-dihydroxy-1,4-benzoquinonato ligands are positioned closer to an edge-to-edge orientation, yielding a quadrangular frustum of a pyramid. The distance between the two proximal chlorine atoms on opposite ligands (d_1) is about 3.638 Å (Table 1). The distances between the two distal chlorine atoms on opposite ligands (d_2) and the two "naked" nitrogen atoms are nearly the same, being 8.376 and 8.302 Å, respectively.

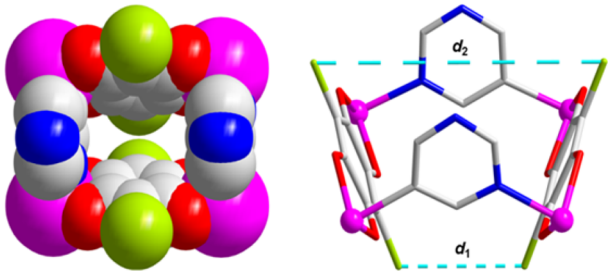

Figure 1. Crystallographically derived structure of heteroarylrhodium complex **3**. POV-Ray depictions of the molecular structures of heteroarylrhodium complex **3** in the solid state. C, gray; N, blue; O, red; Cl, lime; Rh, pink. H-atoms and triflate are omitted for clarity.

Table 1. Structure Data[a]

	Ag−Ag (Å)	d_1 (Å)	d_2 (Å)	d_3 (Å)
complex **3**		3.638	8.376	
capsule **4**	7.587	3.557	8.643	4.439
p-xyleneC**4**	6.641	3.543	9.054	4.595
p-dibromobenzeneC**4**	7.136	3.509	8.922	3.715, 5.151
pCpC**4**	9.231	3.380	8.812	4.481

[a] d_1 is the distance between the two proximal chlorine atoms on opposite ligands, d_2 is the distance between the two distal chlorine atoms on opposite ligands, and d_3 is the distance between the two proximal chlorine atoms pointing inward toward the cavity. See Figures 1 and 2.

Formation of Heterometallic Capsule 4. It was expected that the "naked" nitrogen atoms of the pyrimidine moieties at the convex of **3** could further accommodate two metal ions to give a heterometallic capsule **4** (Figure 2a). Heterometallic capsule **4** was isolated in 95% yield by stirring complex **3** for 24 h in the presence of AgOTf in CD_3OD and subsequent recrystallization by diethyl ether vapor diffusion in the dark. The ^{1}H NMR signals of the pyrimidyl groups were gradually shifted downfield, which indicated the coordination of the silver(I) ions to the residual nitrogen atoms of the complex **3** (Figure 2b,c). In addition, the signals of Cp* rings were also shifted downfield slightly in the ^{1}H NMR spectra. In the CSI-TOF-MS spectrum of capsule **4**, the peaks at m/z = 1930.29 and m/z = 1237.20, corresponding to $[\mathbf{4} - 2\text{OTf}]^{2+}$ and $[\mathbf{4} - 3\text{OTf}]^{3+}$ species, respectively, were observed, and their isotopic resolutions are in good agreement with theoretical distributions (Figure S3).

Complex **4** has been structurally characterized and displays the expected tube-like $[Rh_8Ag_2]$ structure. As shown in Figures 2d,e, two molecules of **3** were connected via coordination of silver to the pyrimidine nitrogen atoms in a linear geometry. Thus, a molecular capsule was formed through metal ions as metal "hinges". The N−Ag−N angle is 177.7°. The Ag···Ag separation of 7.587 Å, and the distance of 14.676 Å between the two most distant Rh(III) ions, result in a narrow tubular capsule (Table 1).

Encapsulation of Guest Molecules with Capsule 4. ^{1}H NMR spectroscopy gave a clear indication of the interaction of *p*-xylene and capsule **4** (Figures 3a−c). When excess *p*-xylene was added to a CD_3OD solution of capsule **4**, the signals of the original capsule **4** were replaced by a new set of signals in the aromatic region. In addition to the signals of free *p*-xylene at 7.03 and 2.27 ppm, the new signals at 6.48 ppm and −0.69 ppm can be assigned as those of included *p*-xylene, which are highly upfield shifted due to the strong shielding effect of the cavity. The large upfield shift of the methyl group ($\Delta\delta$ = −2.96 ppm) is presumably due to the methyl groups being positioned deep

DOI: 10.1021/jacs.6b06622
J. Am. Chem. Soc. 2016, 138, 10700−10707

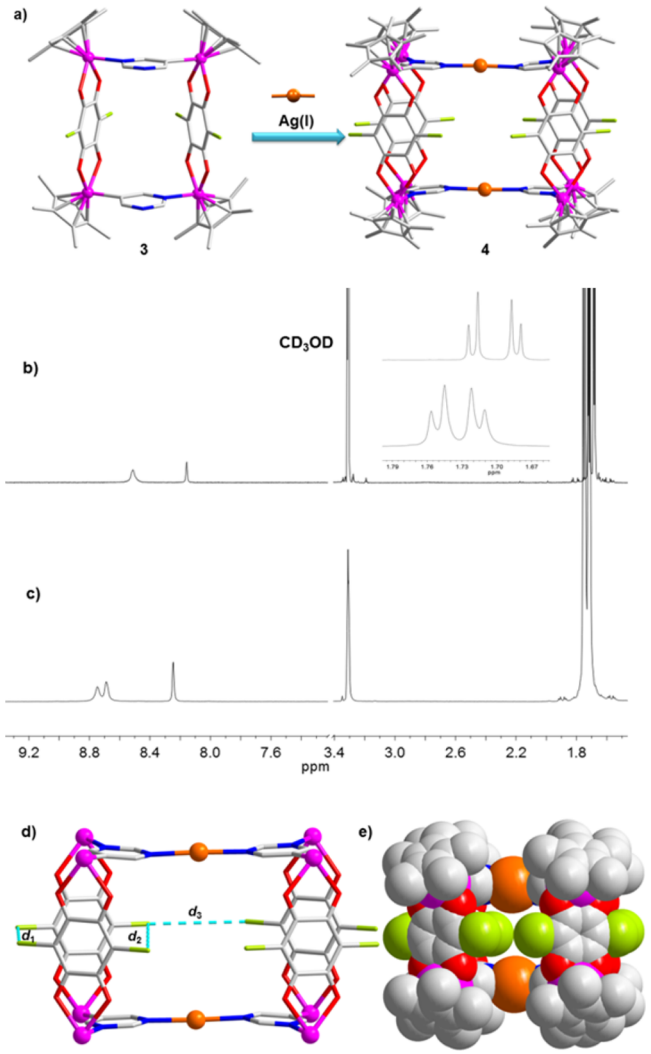

Figure 2. Formation and characterization of **4**. (a) Cartoon illustration of the metal-triggered structural switching from **3** to **4**. (b,c) ^{1}H NMR spectra (400 MHz, room temperature, CD_3OD) of complexes of (b) metallarectangle **3** and (c) capsule **4**. (d,e) Crystallographically derived structure of **4**: (d) wire representation (Cp* rings, counterions, and solvents are omitted for clarity) and (e) space-filling representation (counterions and solvent molecules are omitted for clarity).

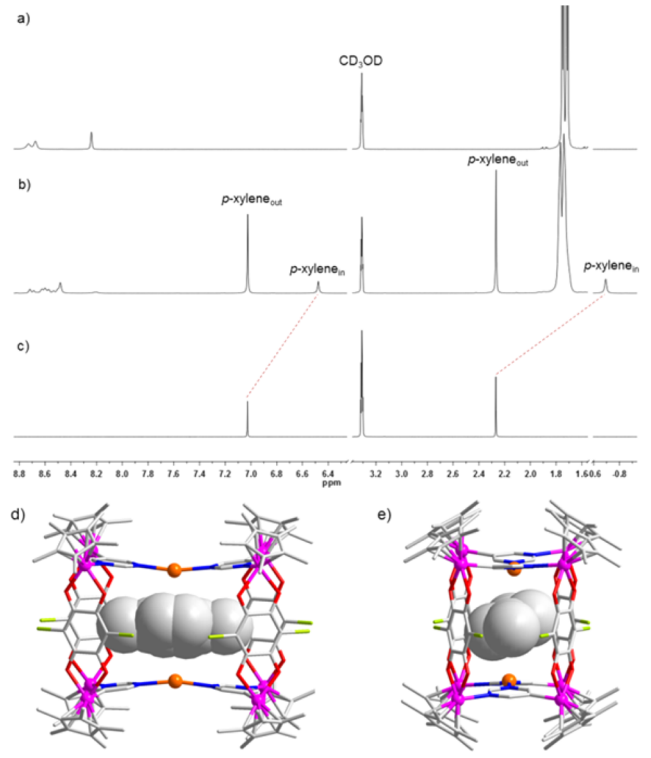

Figure 3. Formation and characterization of *p*-xylene⊂ **4**. (a–c) ^{1}H NMR spectra (400 MHz, 300 K) of **4** (C = 9.0 mM) in the presence of (a) 0.0 and (b) 4.0 equiv of *p*-xylene and (c) *p*-xylene in CD_3OD without the complex. (d,e) Two views of the crystallographically derived structure of *p*-xylene⊂**4**: cylindrical (for **4**) and space-filling (for *p*-xylene) representations. Counterions and solvent molecules are omitted for clarity.

in the cavity, near the aromatic rings. Diffusion-ordered NMR spectroscopy (DOSY) revealed the formation of a host–guest assembly (Figure S4). This conjecture is supported by the structure in the solid state (Figures 3d,e). In order to determine the exchange rate of the guest, the experiments of variable-temperature ^{1}H NMR (Figure S5) and NMR exchange spectroscopy (EXSY) on the titration sample containing 4 equiv of *p*-xylene were performed.[S4] The exchange rate constant of the guest as $k \approx 1.27$ s^{-1} for *p*-xylene⊂**4** was estimated by a 2D EXSY experiment at 298 K (Figure S6).

Single crystals of *p*-xylene⊂**4** suitable for X-ray structure determination were grown by slow vapor diffusion of diethyl ether into a methanol solution of the capsule **4** in the presence of excess *p*-xylene. In the resulting structure, one disordered *p*-xylene was found to reside in the cavity of capsule **4** via an η^2-type Ag–π interaction at each edge of the benzene ring (i.e., the C_2–C_3 and C_5–C_6 bonds). The two methyl groups are held in the two aromatic cavities, in agreement with the unusually upfield shifts observed in the ^{1}H NMR spectra. Multipoint CH–π interactions between the methyl groups and the bridging 2,5-dichloro-3,6-dihydroxy-1,4-benzoquinonato and pyrimidine rings appear to stabilize the complex, with CH–π distances of around 2.87 Å. The average Ag–C distance is 3.14 Å, indicating relatively weak Ag–π interactions (Table 1). As a result of the *p*-xylene encapsulation, the capsule structure is compressed and the Ag–Ag distance is decreased to 6.641 Å; however, the Cl–Cl distances of the central pocket are increased to 4.595 Å (d_2) and 9.054 Å (d_3). Thus, the capsule seems to be able to tune its size and shape to accept the guest molecule. This conformational flexibility may provide the possibility for the present capsule to allow the relatively different organic compounds to enter its nanocavity.

Subsequently, we explored the ability of the capsule for the encapsulation of a series of dihalogenated benzene derivatives. For instance, when a mixture of capsule **4** and excess *p*-dibromobenzene in methanol was stirred at room temperature for 5 min, host–guest complex *p*-dibromobenzene⊂**4** was formed. The encapsulated process was unambiguously verified by NMR spectroscopy (Figure S7). Dramatic changes in the ^{1}H NMR spectra were observed upon addition of excess *p*-dibromobenzene to a solution of capsule **4** in CD_3OD. The signal of the encapsulated guest is shifted upfield by 0.64 ppm with respect to that of the free *p*-dibromobenzene due to the shielding effect of the capsule. DOSY revealed the formation of a single host–guest assembly, as all the proton signals showed the same diffusion coefficient (Figure S8). Variable-temperature ^{1}H NMR study on the titration sample containing 2.0 equiv of *p*-dibromobenzene indicated that the guest exchange becomes

DOI: 10.1021/jacs.6b06622
J. Am. Chem. Soc. 2016, 138, 10700–10707

faster upon heating the above solution to 313 K (Figure S9). An 2D EXSY experiment of a 2:1 sample of *p*-dibromobenzene and empty capsule **4** was employed to determine the exchange rate of the guest as $k \approx 0.79\ s^{-1}$ (Figure S10). The CSI-TOF-MS spectrum of the product clearly supports the formation of host–guest system *p*-dibromobenzene⊂**4**, and the experimental isotopic patterns are in agreement with the calculated peak distributions (Figure S11).

By diethyl ether vapor diffusion into a mixture of **4** and 1.0 equiv of *p*-dibromobenzene in methanol in the dark, red single crystals were obtained in 99% yield based on capsule **4**. Crystallographic analysis of *p*-dibromobenzene⊂**4** confirmed that the guest molecule *p*-dibromobenzene occupies the cavity of the capsule **4** (Figure 4 and Table 1). The crystal structure

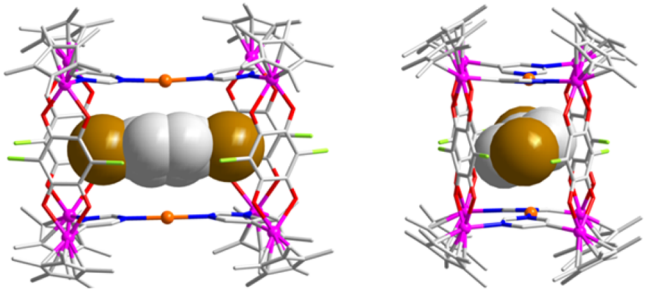

Figure 4. Two views of the crystallographically derived structure of *p*-dibromobenzene⊂**4**: cylindrical (for **4**) and space-filling (for *p*-dibromobenzene) representations. Counterions and solvent molecules are omitted for clarity.

also revealed the encapsulated *p*-dibromobenzene guest adopts an tilted configuration, allowing for the formation of η^2-type Ag–π interactions (Ag–C 3.40–3.45 Å) to stabilize the final structure. The resulting Ag–π arrangement with the phenylene ring is quite similar to that of the above-mentioned *p*-xylene inclusion complex. In addition, weak noncovalent anion–π interactions were also observed between the bromide groups and the capsule pocket.

Similar to *p*-dibromobenzene, the slightly smaller and larger dihalogenated benzene derivatives *p*-dichlorobenzene and *p*-diiodobenzene, respectively, were found to occupy the cavity of capsule **4**. In each of these cases, the ^{1}H NMR spectra revealed that the aromatic C–H signal of the encapsulated guest had shifted from the signal of the free molecule, indicating the inclusion of the guest in the cavity (Figures S12 and S14). DOSY NMR experiments afforded a similar hydrodynamic radii for both inclusion complexes when compared with that of the *p*-xylene⊂**4** or *p*-dibromobenzene⊂**4**, demonstrating that the size of the molecular entities is nearly identical (Figures S13 and S15). 2D EXSY experiments of a 1:1 sample of *p*-dichlorobenzene or *p*-diiodobenzene and empty capsule **4** was used to determine the exchange rate of the guests as $k \approx 3.06\ s^{-1}$ for *p*-dichlorobenzene⊂**4** and $k \approx 1.65\ s^{-1}$ for *p*-diiodobenzene⊂**4**, respectively (Figures S16 and S17).

In the above-mentioned examples, we found that the capsule can easily make adjustments along all the directions with available free space to fit the target molecules. The observation suggested the capability of the capsule to change its cavity to form the required structure. We then explored the encapsulation of [2.2]paracyclophane (pCp) with capsule **4** following a similar procedure as for *p*-dibromobenzene. Upon addition of pCp to a solution of capsule **4** in CD_3OD at room temperature, the signals of the host molecule were obviously shifted due to host–guest interactions (Figure 5a–c). Due to

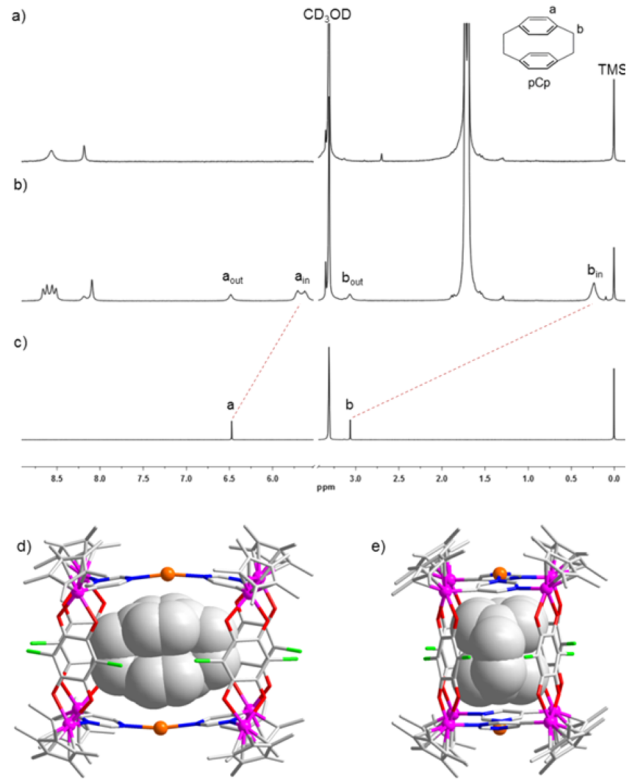

Figure 5. Formation and characterization of pCp⊂**4**. (a–c) ^{1}H NMR spectra (400 MHz, 300 K) of **4** (C = 4.0 mM) in the presence of (a) 0.0 and (b) 3.0 equiv of pCp and (c) only pCp in CD_3OD without the complex. (d,e) Two views of the crystallographically derived structure of pCp⊂**4**: cylindrical (for **4**) and space-filling (for pCp) representations. Counterions and solvent molecules are omitted for clarity.

the strong shielding effect of the cavity, the signals corresponding to the included pCp were significantly upfield shifted ($\Delta\delta$ = −0.81 and −2.83 for a_{in} and b_{in}, respectively). This assignment was strongly supported by its single-crystal X-ray analysis. As shown in Figure 5d,e, crystallographic analysis of pCp⊂**4** confirmed that one pCp molecule guest was included in the cavity of the capsule. The Ag–Ag distance was enlarged to 9.231 Å in order to accommodate pCp (Table 1). The crystal structure also revealed the formation of the stacked Ag–π–π–Ag configuration. 2D DOSY NMR spectroscopic results indicated that the same inclusion complex is formed in solution and in the solid state (Figure S18). Based on 2D EXSY experiment at 298 K, the exchange rate constant of the guest was found to be $k \approx 0.68\ s^{-1}$ (Figure S19).

Comparison of crystallographic data for capsule **4**, *p*-xylene⊂**4**, *p*-dibromobenzene⊂**4**, and pCp⊂**4** shows that the Ag–Ag interdistance is ca. 7.6 Å when the guest molecule is absent, whereas the inclusion of *p*-dibromobenzene compresses this distance about 5.9%, and inclusion of *p*-xylene further shrinks it by about 6.5% (total: 12.4% compares to free capsule). The inclusion of the pCp molecule enlarges this distance about 21.7% longer than the empty complex. The change of cavity size in the process of accommodating guest molecules indicates that the flexibility of capsule **4**, owing to the silver hinges in the

DOI: 10.1021/jacs.6b06622
J. Am. Chem. Soc. 2016, 138, 10700–10707

bridge positions, allows the capsule to fine-tune the size of the cavity to maximize its interaction with the guest species.

Selective Encapsulation of Isomers by Capsule 4. Remarkably, the capsule **4** was found to selectively bind *p*-xylene over its isomers, such as *m*-xylene, *o*-xylene, and ethylbenzene (Figures S20–S22). As indicated by NMR spectroscopy, addition of an excess of either *m*-xylene, *o*-xylene, or ethylbenzene to a solution of capsule **4** in CD_3OD showed no change relative to the signals of the free capsule and aromatic molecule. On the other hand, when an equimolar mixture containing *p*-xylene, *m*-xylene, *o*-xylene, and ethylbenzene was added to the solution of capsule **4**, the formation of the host–guest system *p*-xylene⊂**4** is exclusively observed (Figure S23). We hypothesize that the tight fit of the molecule and the existence of Ag–π interactions are essential to the encapsulation. To further verify the size/shape selectivity of the capsule, we then explored the separation of isomeric dihalogenated benzene derivatives with capsule **4** following a similar procedure as that used for the xylenes. The selective binding with *p*-dibromobenzene with respect to other isomers (*m*-dibromobenzene or *o*-dibromobenzene) was also investigated via NMR spectroscopy (Figures S24 and S25), using a mixture of capsule **4** with 1 molar equivalent of *p*-dibromobenzene and 4 molar equivalents each of *m*-dibromobenzene and *o*-dibromobenzene in a CD_3OD solution. The ^1H NMR spectra showed exclusive encapsulation of *p*-dibromobenzene with disappearance of the signal for free *p*-dibromobenzene, accompanied by a new signal observed at high field (Figure S26), while the signals belonging to the other free isomers were unchanged. Similar to *p*-xylene, the selective encapsulation of *p*-dichlorobenzene or *p*-diiodobenzene from their corresponding isomers was also realized (Figures S27 and S28). To estimate the contribution of capsule structure on the stability of the inclusion complex, control experiments were then performed. When an excess amount of guest was added to a methanol solution of the silver-free complex **3**, its ^1H NMR spectrum did not show any change, suggesting very weak interactions between the guest and complex **3** (Figure S29). On the other hand, no significant changes were observed when AgOTf was combined with the guest molecules, such as pCp (Figure S30).

Release of Guest Molecules from Capsule 4. The release of the captured guest molecules from the capsule was also investigated. We were delighted to find that all encapsulated *p*-xylene can be extracted by washing with excess diethyl ether from the obtained solid sample *p*-xylene⊂**4**. The regeneration of empty capsule **4′** was confirmed by the single-crystal structural analysis (Table S1). The remaining solid can be used for further encapsulation of *p*-xylene from mixture following the above-mentioned procedure. However, a similar protocol aimed at liberating encapsulated dihalogenated benzene derivatives or pCp was unsuccessful. We therefore decided to seek other methods for guest liberation from the host–guest adducts. The first method was removal of metal ions using halide salts such as NaCl to disassemble the capsule. Upon addition of two equivalents of NaCl to a solution of *p*-diiodobenzene⊂**4** in CD_3OD at room temperature for 10 min, the signal corresponding to the encapsulated guest disappeared, indicating release of *p*-diiodobenzene from the capsule. The disassembly of capsule **4** and a structural rearrangement to metallacycle **3** were found to occur, as indicated by ^1H NMR spectra. The solvent was removed after filtration and *p*-diiodobenzene was extracted with diethyl ether and isolated in 98% yield based on *p*-diiodobenzene⊂**4**. After the addition of NaCl to *p*-diiodobenzene⊂**4** in CD_3OD, *p*-diiodobenzene⊂**4** was regenerated in nearly quantitative yield from the suspended mixture of **3** and *p*-diiodobenzene by addition of AgOTf at room temperature (Figure 6). The captured *p*-diiodobenzene guest can also be released as the host dissembles upon external stimulation with sunlight, as indicated by NMR experiment (Figure S31). Exposure of the solution of *p*-diiodobenzene⊂**4** to sunlight at room temperature for 3 h resulted in the signal of *p*-diiodobenzene encapsulated in **4** disappeared, completely, indicating the release of guest from the capsule. Complex **3** was isolated in 91% recovery based on *p*-diiodobenzene⊂**4**.

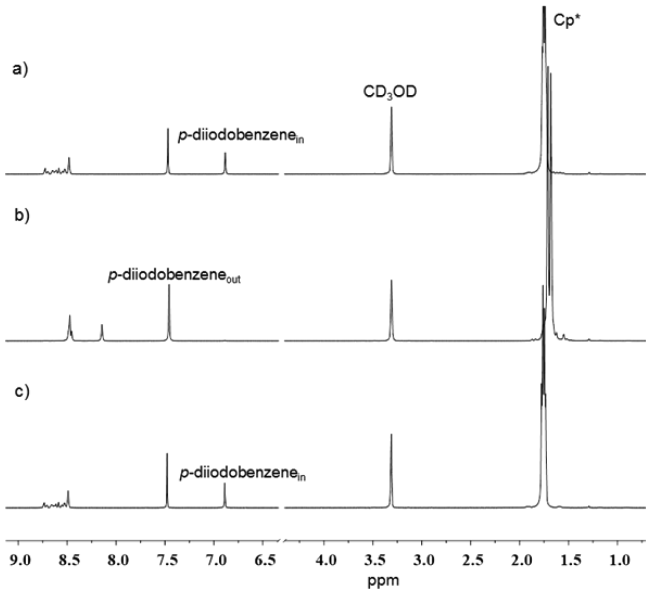

Figure 6. Partial NMR in situ detection of the uptake and release of *p*-diiodobenzene in the host capsule (400 MHz, 300 K, CD_3OD): (a) complex **4** (C = 4.5 mM) in the presence of 2.2 equiv of *p*-diiodobenzene, (b) addition of 2.2 equiv of NaCl to the solution from (a), and (c) addition of 2.2 equiv of AgOTf to the solution from (b).

CONCLUDING REMARKS

In general, we have shown that the present heterometallic capsule **4** is not only suitable as a host for the encapsulation of a series of aromatic compounds, the receptor also shows widely differing specificity for the various isomers. Based on the presented experimental data we proposed that the size and shape matching, as well as the metal–π interactions, are the main forces governing the extent of molecular recognition. These results showcase an attractive methodology to selectively extract one isomer from mixtures, providing a platform to design tuned capsules for selective recognition of specific target molecules. The selected guest can then be released by using a simple solid–liquid solvent washing strategy or an external light stimulus. It is worth noting that the *p*-xylene is always produced together with *m*-xylene, *o*-xylene, and ethylbenzene in industry, and the selective separation of *p*-xylene from the mixture is still a challenge. Our present catch-and-release procedure provides a potential method to resolve this problem. We wish these findings may spark supramolecular host–guest research in the separation of regioisomeric compounds, and it might be useful in separation of very high value isomeric molecules, such as isotopically labeled or radioactive derivatives.

DOI: 10.1021/jacs.6b06622
J. Am. Chem. Soc. 2016, 138, 10700–10707

EXPERIMENTAL SECTION

General Procedures. All experiments were conducted under nitrogen using standard Schlenk techniques. Unless otherwise stated, all commercial reagents and solvents were used as obtained without additional purification. NMR spectra (^{1}H, ^{13}C{^{1}H}, and ^{1}H,^{1}H COSY, 2D DOSY) were recorded on Bruker AVANCE I 400 or Bruker AVANCE III 400 spectrometers. 2D EXSY was measured on Bruker AVANCE 500 spectrometers. Chemical shifts (δ) are expressed in ppm downfield from tetramethylsilane using the residual protonated solvent as an internal standard. Mass spectra were obtained with MicroTof (Bruker Daltonics, Bremen), or API-TOF-MS 10000 (HEXIN, Beijing) spectrometers. Syntheses and characterization for complex **2** are given in the Supporting Information. *The efficient full $^{13}C\{^1H\}$ NMR spectrum for these complexes cannot be obtained due to its limited solubility even after 24 h.*

Preparation of 3. AgOTf (28 mg, 0.11 mmol) was added to a solution of $[Cp^*_2Rh_2(\mu\text{-CA})]Cl_2$ (38 mg, 0.05 mmol) in CH_3OH/H_2O (10 mL, 10:1) at room temperature. The reaction mixture immediately turned grass-green, and white solid AgCl precipitated from the solution over the course of 10 min. The obtained suspension was filtered. 5-Pyrimidine boronic acid (24 mg, 0.2 mmol) was added to the filtrate. The mixture was stirred at room temperature for 24 h. The reaction mixture was concentrated to a volume of 3 mL under reduced pressure, filtered through Celite and recrystallized under slow diethyl ether diffusion into the filtrate. A red crystalline solid was obtained (37 mg, 82%). ^{1}H NMR (400 MHz, CD_3OD, ppm): δ = 1.68−1.73 (60H, Cp*), 8.15 (2H, Ar−H), 8.47 (br, 4H, Ar−H). Anal. Calcd for $C_{62}H_{66}Cl_4F_6N_4O_{14}Rh_4S_2$: C 40.85, H 3.65, N 3.07, found: C 40.59, H 3.53, N 3.12. MS (MALDI-TOF, CH_3OH): m/z = 1673 (calcd for $[M - OTf]^+$ 1673).

Preparation of 4. AgOTf (5.2 mg, 0.02 mmol) was added to a solution of **3** (18 mg, 0.01 mmol) in CH_3OH (10 mL) at room temperature. The mixture was stirred at room temperature for 24 h. Crystals of **4** were obtained by diffusion diethyl ether into this solution. The obtained crystals were collected and dried under vacuum (22 mg, 95%). ^{1}H NMR (400 MHz, CD_3OD, ppm): δ = 1.71−1.75 (120H, Cp*), 8.25 (4H, Ar−H), 8.69−8.75 (br, 8H, Ar−H). Anal. Calcd for $C_{126}H_{132}Ag_2Cl_8F_{18}N_8O_{34}Rh_8S_6$: C 36.38, H 3.20, N 2.69, found: C 36.62, H 3.09, N 2.65. MS (CSI-TOF, CH_3OH): m/z = 1237.20 (calcd for $[M - 3OTf]^{3+}$ 1237.21), 1930.29 (calcd for $[M - 2OTf]^{2+}$ 1930.29).

General Method for the Study of Host−Guest Chemistry. Host−guest interactions in solution were studied by NMR spectroscopy. The experiments between capsule **4** and the different guest molecules were performed using CD_3OD as solvent. Excess guest was used in each case. The corresponding guest molecule (excess) was added to a CD_3OD (0.5 mL) solution of capsule **4** (4.5 μmol) in a brown glass NMR tube. The mixture was stirred at room temperature for 1 min. The process was monitored by NMR spectroscopy. Whereas no binding with capsule **4** was observed when *o*-xylene, *m*-xylene, *o*-dichlorobenzene, *m*-dichlorobenzene, *o*-dibromobenzene, *m*-dibromobenzene, *o*-diiodobenzene, *m*-diiodobenzene, 1,2-diphenylethyne, or naphthalene was used, the addition of *p*-xylene, *p*-dichlorobenzene, *p*-dibromobenzene, *p*-diiodobenzene or pCp led to shifts in the ^{1}H NMR spectrum of **4**. No binding with was observed capsule **4** for dichloromethane, chloroform, dichloroethane, 1,2-dimethoxyethane, or hexane molecules.

Preparation of Guest⊂4. *p-Xylene⊂4.* *p*-Xylene (2.25 μL, 9 μmol) was added to a methanol solution of capsule **4** (9.5 mg, 2.3 μmol), the mixture was stirred at room temperature for 5 min. The mixture was filtered, and the crystals were obtained by diethyl ether diffusion into the solution in the dark for few of days. The inclusion complex was isolated as red solids (9.5 mg, 98%). ^{1}H NMR (400 MHz, CD_3OD, ppm): δ = −0.69 (*p*-xylene), 1.73−1.78 (120H, Cp*), 6.48 (s, *p*-xylene), 8.48−8.72 (br, 12H, Ar−H).

p-Dichlorobenzene⊂4. *p*-Dichlorobenzene (0.8 mg, 5.5 μmol) was added to a methanol solution of capsule **4** (9.5 mg, 2.3 μmol), the mixture was stirred at room temperature for 5 min. The mixture was filtered. Diethyl ether was added to the solution, and the product was isolated by filtration and dried under vacuum (9.7 mg, 98%). ^{1}H NMR (400 MHz, CD_3OD, ppm): δ = 1.74−1.78 (120H, Cp*), 6.69 (4H, inside *p*-dichlorobenzene H), 8.46−8.73 (12H, PymH).

p-Dibromobenzene⊂4. *p*-Dibromobenzene (1.0 mg, 4.6 μmol) was added to a methanol solution of capsule **4** (9.5 mg, 2.3 μmol), the mixture was stirred at room temperature for 5 min. The mixture was filtered. Diethyl ether was added to the solution, and the product was isolated by filtration and dried under vacuum. (10.1 mg, 99%). ^{1}H NMR (400 MHz, CD_3OD, ppm): δ = 1.74−1.78 (120H, Cp*), 6.80 (s, 4H, *p*-dibromobenzene), 8.47−8.73 (12H, Ar−H). Anal. Calcd for $C_{132}H_{136}Ag_2Br_2Cl_8F_{18}N_8O_{34}Rh_8S_6$: C 36.07, H 3.12, N 2.55, found: C 36.06, H 3.00, N 2.50. MS (CSI-TOF, CH_3OH): m/z = 949.63 (calcd for $[M - 4OTf]^{4+}$ 949.64), 1315.85 (calcd for $[M - 3OTf]^{3+}$ 1315.83).

p-Diiodobenzene⊂4. *p*-Diiodobenzene solid (1.3 mg, 3.6 μmol) was added to a methanol solution of capsule **4** (9.5 mg, 2.3 μmol), the mixture was stirred at room temperature for 5 min. The mixture was filtered. Diethyl ether was added to the solution, and the product was isolated by filtration and dried under vacuum (10.0 mg, 97%). ^{1}H NMR (400 MHz, CD_3OD, ppm): δ = 1.74−1.78 (120H, Cp*), 6.89 (s, 4H, *p*-diiodobenzene), 8.49−8.74 (12H, Ar−H).

pCp⊂4. Compound pCp (1.2 mg, 6.0 μmol) was added to a methanol solution of capsule **4** (9.5 mg, 2.3 μmol), the mixture was stirred at room temperature for 5 min. The mixture was filtered. Diethyl ether was added to the solution, and the product was isolated by filtration and dried under vacuum (8.0 mg, 92%). ^{1}H NMR (400 MHz, CD_3OD, ppm): δ = 0.24 (8H, pCp, methylene-H), 1.69−1.73 (120H, Cp*), 5.71−5.63 (8H, pCp, Ar−H), 8.10 (4H, Ar−H), 8.51−8.66 (8H, Ar−H). Anal. Calcd for $C_{142}H_{148}Ag_2Cl_8F_{18}N_8O_{34}Rh_8S_6$: C 39.05, H 3.42, N 2.57, found: C 38.89, H 3.76, N 2.42.

Removal of Silver Ions and Release of Guest from *p*-Diiodobenzene⊂4. Method 1: To a stirred solution of *p*-diiodobenzene⊂**4** (2.3 μmol, in order to facilitate the comparison the encapsulated and free guest, excess *p*-diiodobenzene was used) in methanol (2 mL), NaCl or NH_4Cl (9.2 μmol) was added. The suspension was stirred for 10 min and then filtered. Red crystalline product was obtained by slow diffusion diethyl ether into the filtrate, the solid was collected, washed with diethyl ether and dried under vacuum. ^{1}H NMR experiment of the products revealed the formation of the metallarectangle **3** (98%, based on *p*-diiodobenzene⊂**4**). Method 2: Exposure of the solution of *p*-diiodobenzene⊂**4** (2.3 μmol) in methanol under sunlight at room temperature for 3 h produced a powdery suspension of solids. The solvent was removed under vacuum, and then the solid was washed by chloroform and diethyl ether, the solid was dissolved in methanol and then filtered. Red crystalline product was obtained by slow diffusion diethyl ether into the obtained filtrate, the solid was collected, washed with diethyl ether and dried under vacuum. ^{1}H NMR experiment of the isolated solids revealed the formation of the metallarectangle **3** (91%, based on *p*-diiodobenzene⊂**4**). A similar method was used for the release of *p*-dibromobenzene or *p*-dichlorobenzene.

X-ray Crystallography Details. Crystallographic data for complexes **3**, **4**, and **4′** were collected at 173 K using a CCD-Bruker APEX DUO system (Mo Kα, λ = 0.71073 Å). Crystallographic data for complexes *p*-xylene⊂**4**, *p*-dibromobenzene⊂**4**, and pCp⊂**4** were collected at 150 K using a Bruker D8 VENTURE microfocus X-ray sources system (Cu Kα, λ = 1.54178 Å). Indexing was performed using APEX 2 (difference vectors method). Data integration and reduction were performed using SaintPlus 6.01. Absorption correction was performed by the multiscan method implemented in SADABS. The structures were solved and refined using SHELXTL-97 (for complexes **3**, **4**, and **4′**) or SHELXTL-2014 (complexes *p*-xylene⊂**4**, *p*-dibromobenzene⊂**4**, and pCp⊂**4**) contained in the SHELXTL program.[55] In complexes **4**, *p*-xylene⊂**4**, *p*-dibromobenzene⊂**4**, and pCp⊂**4**, there are disordered anions and solvent molecules which could not be restrained properly. Therefore, the SQUEEZE algorithm was used. Additional details, including CIF files, can be found in the Supporting Information.

DOI: 10.1021/jacs.6b06622
J. Am. Chem. Soc. 2016, 138, 10700−10707

■ ASSOCIATED CONTENT

Supporting Information

The Supporting Information is available free of charge on the ACS Publications website at DOI: 10.1021/jacs.6b06622.

Synthesis and characterization details of complex **2**, NMR experimental spectra, MS spectra, structure refinement details, and tables of crystal data for all complexes, including Figures S1−S31, Table S1, and Table S2 (PDF)

X-ray crystallographic files for **2** (CIF)

X-ray crystallographic files for **3** (CIF)

X-ray crystallographic files for **4** (CIF)

X-ray crystallographic files for pCp⊂**4** (CIF)

X-ray crystallographic files for *p*-dibromobenzene⊂**4** (CIF)

X-ray crystallographic files for *p*-xylene⊂**4** (CIF)

■ AUTHOR INFORMATION

Corresponding Authors

*yfhan1980@fudan.edu.cn

*gxjin@fudan.edu.cn

Notes

The authors declare no competing financial interest.

■ ACKNOWLEDGMENTS

Dedicated to Professor Max Herberhold on the occasion of his 80th birthday. We thank J.-P. Huang and Prof. J. M. He for measuring the CSI-TOF-MS spectra of **4** and *p*-dibromobenzene⊂**4**. This work was supported by grants from the National Natural Science Foundation of China (21371036, 21531002, 21374019), the Program for Changjiang Scholars and Innovative Research Team (IRT1117), the Shanghai Pujiang Program (14PJD006), and the Shanghai Science and Technology Committee (13JC1400600, 13DZ2275200).

■ REFERENCES

(1) Méthivier, A. *Zeolites for cleaner technologies*; Imperial College Press: London, 2002.

(2) Li, J.-R.; Sculley, J.; Zhou, H.-C. *Chem. Rev.* **2012**, *112*, 869−932.

(3) Van de Voorde, B.; Bueken, B.; Denayer, J.; De Vos, D. *Chem. Soc. Rev.* **2014**, *43*, 5766−5788.

(4) Gu, Z.-Y.; Yang, C.-X.; Chang, N.; Yan, X.-P. *Acc. Chem. Res.* **2012**, *45*, 734−745.

(5) Herm, Z. R.; Bloch, E. D.; Long, J. R. *Chem. Mater.* **2014**, *26*, 323−338.

(6) Furukawa, H.; Cordova, K. E.; O'Keeffe, M.; Yaghi, O. M. *Science* **2013**, *341*, 974−985.

(7) Farha, O. K.; Eryazici, I.; Jeong, N. C.; Hauser, B. G.; Wilmer, C. E.; Sarjeant, A. A.; Snurr, R. Q.; Nguyen, S. T.; Yazaydın, A. Ö.; Hupp, J. T. *J. Am. Chem. Soc.* **2012**, *134*, 15016−15021.

(8) Horike, S.; Shimomura, S.; Kitagawa, S. *Nat. Chem.* **2009**, *1*, 695−704.

(9) (a) Férey, G.; Serre, C. *Chem. Soc. Rev.* **2009**, *38*, 1380−1399. (b) Bradshaw, D.; Claridge, J. B.; Cussen, E. J.; Prior, T. J.; Rosseinsky, M. J. *Acc. Chem. Res.* **2005**, *38*, 273−282.

(10) Schneemann, A.; Bon, V.; Schwedler, I.; Senkovska, I.; Kaskel, S.; Fischer, R. A. *Chem. Soc. Rev.* **2014**, *43*, 6062−6096.

(11) Krishna, R. *Phys. Chem. Chem. Phys.* **2015**, *17*, 39−59.

(12) Xomeritakis, G.; Lai, Z.; Tsapatsis, M. *Ind. Eng. Chem. Res.* **2001**, *40*, 544−552.

(13) Rana, M.; Reddy, R. B.; Rath, B. B.; Gautam, U. K. *Angew. Chem., Int. Ed.* **2014**, *53*, 13523−13527.

(14) Gu, Z.-Y.; Yan, X.-P. *Angew. Chem., Int. Ed.* **2010**, *49*, 1477−1480.

(15) El Osta, R.; Carlin-Sinclair, A.; Guillou, N.; Walton, R. I.; Vermoortele, F.; Maes, M.; de Vos, D.; Millange, F. *Chem. Mater.* **2012**, *24*, 2781−2791.

(16) Fang, Z.-L.; Zheng, S.-R.; Tan, J.-B.; Cai, S.-L.; Fan, J.; Yan, X.; Zhang, W.-G. *J. Chromatogr. A* **2013**, *1285*, 132−138.

(17) Nicolau, M. P. M.; Bárcia, P. S.; Gallegos, J. M.; Silva, J. A. C.; Rodrigues, A. E.; Chen, B. *J. Phys. Chem. C* **2009**, *113*, 13173−13179.

(18) Moreira, M. A.; Santos, J. C.; Ferreira, A. F. P.; Loureiro, J. M.; Ragon, F.; Horcajada, P.; Shim, K.-E.; Hwang, Y.-K.; Lee, U.-H.; Chang, J.-S.; Serre, C.; Rodrigues, A. E. *Langmuir* **2012**, *28*, 5715−5723.

(19) Jin, Z.; Zhao, H.-Y.; Zhao, X.-J.; Fang, Q.-R.; Long, J. R.; Zhu, G.-S. *Chem. Commun.* **2010**, *46*, 8612−8614.

(20) Mukherjee, S.; Joarder, B.; Manna, B.; Desai, A. V.; Chaudhari, A. K.; Ghosh, S. K. *Sci. Rep.* **2014**, *4*, 5761−5767.

(21) Finsy, V.; Verelst, H.; Alaerts, L.; De Vos, D.; Jacobs, P. A.; Baron, G. V.; Denayer, J. F. M. *J. Am. Chem. Soc.* **2008**, *130*, 7110−7118.

(22) Alaerts, L.; Kirschhock, C. E. A.; Maes, M.; van der Veen, M. A.; Finsy, V.; Depla, A.; Martens, J. A.; Baron, G. V.; Jacobs, P. A.; Denayer, J. F. M.; De Vos, D. E. *Angew. Chem., Int. Ed.* **2007**, *46*, 4293−4297.

(23) Vermoortele, F.; Maes, M.; Moghadam, P. Z.; Lennox, M. J.; Ragon, F.; Boulhout, M.; Biswas, S.; Laurier, K. G. M.; Beurroies, I.; Denoyel, R.; Roeffaers, M.; Stock, N.; Düren, T.; Serre, C.; De Vos, D. E. *J. Am. Chem. Soc.* **2011**, *133*, 18526−18529.

(24) Torres-Knoop, A.; Krishna, R.; Dubbeldam, D. *Angew. Chem., Int. Ed.* **2014**, *53*, 7774−7778.

(25) Lin, J.-M.; He, C.-T.; Liao, P.-Q.; Lin, R.-B.; Zhang, J.-P. *Sci. Rep.* **2015**, *5*, 11537.

(26) Hartlieb, K. J.; Holcroft, J. M.; Moghadam, P. Z.; Vermeulen, N. A.; Algaradah, M. M.; Nassar, M. S.; Botros, Y. Y.; Snurr, R. Q.; Stoddart, J. F. *J. Am. Chem. Soc.* **2016**, *138*, 2292−2301.

(27) He, C.-T.; Jiang, L.; Ye, Z.-M.; Krishna, R.; Zhong, Z.-S.; Liao, P.-Q.; Xu, J.; Ouyang, G.; Zhang, J.-P.; Chen, X.-M. *J. Am. Chem. Soc.* **2015**, *137*, 7217−7223.

(28) (a) Olenyuk, B.; Whiteford, J. A.; Fechtenkotter, A.; Stang, P. J. *Nature* **1999**, *398*, 796−799. (b) Yang, H.-B.; Ghosh, K.; Northrop, B. H.; Zheng, Y.-R.; Lyndon, M. M.; Muddiman, D. C.; Stang, P. J. *J. Am. Chem. Soc.* **2007**, *129*, 14187−14189. (c) Yamashina, M.; Sartin, M. M.; Sei, Y.; Akita, M.; Takeuchi, S.; Tahara, T.; Yoshizawa, M. *J. Am. Chem. Soc.* **2015**, *137*, 9266−9269. (d) Roy, B.; Ghosh, A. K.; Srivastava, S.; D'Silva, P.; Mukherjee, P. S. *J. Am. Chem. Soc.* **2015**, *137*, 11916−11919.

(29) (a) Yoshizawa, M.; Tamura, M.; Fujita, M. *Science* **2006**, *312*, 251−254. (b) Inokuma, Y.; Kawano, M.; Fujita, M. *Nat. Chem.* **2011**, *3*, 349−358.

(30) (a) Mal, P.; Breiner, B.; Rissanen, K.; Nitschke, J. R. *Science* **2009**, *324*, 1697−1699. (b) Wood, C. S.; Ronson, T. K.; Belenguer, A. M.; Holstein, J. J.; Nitschke, J. R. *Nat. Chem.* **2015**, *7*, 354−358.

(31) (a) Hahn, F. E.; Seidel, W. W. *Angew. Chem., Int. Ed. Engl.* **1996**, *34*, 2700−2703. (b) Su, C.-Y.; Cai, Y.-P.; Chen, C.-L.; Smith, M. D.; Kaim, W.; zur Loye, H.-C. *J. Am. Chem. Soc.* **2003**, *125*, 8595−8613. (c) Hahn, F. E.; Offermann, M.; Shulze Isfort, C.; Pape, T.; Frölich, R. *Angew. Chem., Int. Ed.* **2008**, *47*, 6794−6797. Zheng, Y.-R.; Zhao, Z.; Wang, M.; Ghosh, K.; Pollock, J. B.; Cook, T. R.; Stang, P. J. *J. Am. Chem. Soc.* **2010**, *132*, 16873−16882.

(32) (a) Smulders, M. M. J.; Riddell, I. A.; Browne, C.; Nitschke, J. R. *Chem. Soc. Rev.* **2013**, *42*, 1728−1754. (b) Brown, C. J.; Toste, F. D.; Bergman, R. G.; Raymond, K. N. *Chem. Rev.* **2015**, *115*, 3012−3035. (c) Zarra, S.; Wood, D. M.; Roberts, D. A.; Nitschke, J. R. *Chem. Soc. Rev.* **2015**, *44*, 419−432.

(33) Cook, T. R.; Stang, P. J. *Chem. Rev.* **2015**, *115*, 7001−7045.

(34) Han, Y.-F.; Jin, G.-X. *Acc. Chem. Res.* **2014**, *47*, 3571−3579.

(35) (a) Chakrabarty, R.; Mukherjee, P. S.; Stang, P. J. *Chem. Rev.* **2011**, *111*, 6810−6918. (b) Cook, T. R.; Zheng, Y.-R.; Stang, P. J. *Chem. Rev.* **2013**, *113*, 734−777. (c) Han, M.; Engelhard, D. M.; Clever, G. H. *Chem. Soc. Rev.* **2014**, *43*, 1848−1860. (d) Castilla, A.

M.; Ramsay, W. J.; Nitschke, J. R. *Acc. Chem. Res.* **2014**, *47*, 2063−2073.
(36) Meng, W.; Breiner, B.; Rissanen, K.; Thoburn, J. D.; Clegg, J. K.; Nitschke, J. R. *Angew. Chem., Int. Ed.* **2011**, *50*, 3479−3483.
(37) Wu, K.; Li, K.; Hou, Y.-J.; Pan, M.; Zhang, L.-Y.; Chen, L.; Su, C.-Y. *Nat. Commun.* **2016**, *7*, 10487.
(38) Niu, Z.; Fang, S.; Liu, X.; Ma, J.-G.; Ma, S.; Cheng, P. *J. Am. Chem. Soc.* **2015**, *137*, 14873−14876.
(39) Sun, Q.-F.; Iwasa, J.; Ogawa, D.; Ishido, Y.; Sato, S.; Ozeki, T.; Sei, Y.; Yamaguchi, K.; Fujita, M. *Science* **2010**, *328*, 1144−1147.
(40) Maverick, A. W.; Buckingham, S. C.; Yao, Q.; Bradbury, J. R.; Stanley, G. G. *J. Am. Chem. Soc.* **1986**, *108*, 7430−7431.
(41) Schwabacher, A. W.; Lee, J.; Lei, H. *J. Am. Chem. Soc.* **1992**, *114*, 7597−7598.
(42) Lee, J.; Schwabacher, A. W. *J. Am. Chem. Soc.* **1994**, *116*, 8382−8383.
(43) Dias, H. V. R.; Wang, Z.; Jin, W. *Inorg. Chem.* **1997**, *36*, 6205−6215.
(44) Hiraoka, S.; Shiro, M.; Shionoya, M. *J. Am. Chem. Soc.* **2004**, *126*, 1214−1218.
(45) Hiraoka, S.; Harano, K.; Shiro, M.; Shionoya, M. *Angew. Chem., Int. Ed.* **2005**, *44*, 2727−2731.
(46) Nakamura, T.; Ube, H.; Shionoya, M. *Angew. Chem., Int. Ed.* **2013**, *52*, 12096−12100.
(47) Kishi, N.; Akita, M.; Kamiya, M.; Hayashi, S.; Hsu, H.-F.; Yoshizawa, M. *J. Am. Chem. Soc.* **2013**, *135*, 12976−12979.
(48) Munakata, M.; Wu, L. P.; Ning, G. L. *Coord. Chem. Rev.* **2000**, *198*, 171−203.
(49) Omoto, K.; Tashiro, S.; Kuritani, M.; Shionoya, M. *J. Am. Chem. Soc.* **2014**, *136*, 17946−17949.
(50) Lindeman, S. V.; Rathore, R.; Kochi, J. K. *Inorg. Chem.* **2000**, *39*, 5707−5716.
(51) Taylor, I. F., Jr.; Hall, E. A.; Amma, E. L. *J. Am. Chem. Soc.* **1969**, *91*, 5745−5749.
(52) Han, Y.-F.; Jia, W.-G.; Lin, Y.-J.; Jin, G.-X. *Organometallics* **2008**, *27*, 5002−5008.
(53) Shi, Y.; Blum, S. A. *Organometallics* **2011**, *30*, 1776−1779.
(54) Perrin, C. L.; Dwyer, T. J. *Chem. Rev.* **1990**, *90*, 935−967.
(55) Sheldrick, G. *Acta Crystallogr., Sect. A: Found. Crystallogr.* **2008**, *64*, 112−122.

DOI: 10.1021/jacs.6b06622
J. Am. Chem. Soc. 2016, 138, 10700−10707